Mass and radius formulas for low-mass neutron stars

Hajime Sotani[1,*], Kei Iida[2], Kazuhiro Oyamatsu[3], and Akira Ohnishi[1]

[1] *Yukawa Institute for Theoretical Physics, Kyoto University, Kyoto 606-8502, Japan*
[2] *Department of Natural Science, Kochi University, 2-5-1 Akebono-cho, Kochi 780-8520, Japan*
[3] *Department of Human Informatics, Aichi Shukutoku University, 9 Katahira, Nagakute, Aichi 480-1197, Japan*
E-mail: sotani@yukawa.kyoto-u.ac.jp

....

Neutron stars, produced at the death of massive stars, are often regarded as giant neutron-rich nuclei. This picture is especially relevant for low-mass (below about solar mass, $M_\odot$) neutron stars, where non-nucleonic components are not expected to occur. Due to the saturation property of nucleonic matter, leading to the celebrated liquid-drop picture of atomic nuclei, empirical nuclear masses and radii can be approximately expressed as function of atomic mass number. It is, however, not straightforward to express masses and radii of neutron stars even in the low-mass range where the structure is determined by a balance between the pressure of neutron-rich nucleonic matter and the gravity. Such expressions would be of great use given possible simultaneous mass and radius measurements. Here we successfully construct theoretical formulas for the masses and radii of low-mass neutron stars from various models that are consistent with empirical masses and radii of stable nuclei. In this process, we discover a new equation-of-state parameter that characterizes the structure of low-mass neutron stars. This parameter, which plays a key role in connecting the mass-radius relation of the laboratory nuclei to that of the celestial objects, could be constrained from future observations of low-mass neutron stars.

....

Subject Index E32, D41

1. Introduction

Neutron stars have been serving as laboratories to probe the densest and most neutron-rich matter in the Universe. It is generally believed that the outer, low-density part of a neutron star (crust) consists of a body-center-cubic lattice of neutron-rich nuclei, embedded in a gas of electrons and, if any, dripped neutrons, and near normal nuclear density (ρ_0), the nuclei melt into uniform nucleonic matter, which mainly composes the star's core [1]. The equation of state (EOS) of matter in the star, i.e., neutron star matter, has one-to-one correspondence to the star's mass (M) and radius (R) relation via hydrostatic equilibrium. Observational data for M have been accumulated [1, 2], whereas those for R have been recently estimated from observations of thermonuclear X-ray bursts with photospheric radius expansion and thermal spectra from quiescent low-mass X-ray binaries [3–6].

In theoretically describing laboratory nuclei and neutron star matter, it is useful to consider the energy of "nuclear matter," i.e., hypothetical infinite matter, composed of neutrons and of protons that have electric charge switched off. For simplicity, as neutron star matter, we will consider zero-temperature, β equilibrated, charge neutral matter made of real nucleons

Table 1 Nuclear matter EOS parameters

EOS	K_0 (MeV)	L (MeV)	η (MeV)
OI-EOSs	180	31.0	55.7
	180	52.2	78.9
	230	42.6	74.7
	230	73.4	107
	280	54.9	94.5
	280	97.5	139
	360	76.4	128
	360	146	197
Shen	281	114	154
Miyatsu	274	77.1	118
FPS	261	34.9	68.2
SLy4	230	45.9	78.5
BSk19	237	31.9	62.3
BSk20	241	37.4	69.6
BSk21	246	46.6	81.1

and electrons. The EOS of nuclear matter is still uncertain even near ρ_0, while it can be constrained from terrestrial nuclear experiments [7] and neutron star observations [4, 5, 8] via theoretical calculations. It is noteworthy that the candidates for low-mass neutron stars have been discovered in binary systems [9], which could give additional information on the EOS once R is measured.

The energy of uniform nuclear matter can be expanded around the saturation point of symmetric nuclear matter (SNM), i.e., nuclear matter made of the same number of neutrons and protons, with respect to the nucleon number density, n_b, and neutron excess, α, defined as $\alpha \equiv (n_n - n_p)/n_b$, where n_n and n_p denote the neutron and proton number densities. In practice, in the vicinity of the saturation point of SNM at zero temperature, the energy per nucleon, w, of uniform nuclear matter can be written as a function of n_b and α [10], i.e.,

$$w = w_0 + \frac{K_0}{18n_0^2}(n_b - n_0)^2 + \left[S_0 + \frac{L}{3n_0}(n_b - n_0) \right]\alpha^2, \tag{1}$$

where w_0, n_0, and K_0 are the saturation energy, the saturation density, and the incompressibility of SNM, while S_0 and L are associated with the symmetry energy coefficient $S(n_b)$. That is, $S_0 = S(n_0)$ is the symmetry energy coefficient at $n_b = n_0$, while L characterizes the density dependence of the nuclear symmetry energy around $n_b = n_0$, defined as $L = 3n_0(dS/dn_b)_{n_b=n_0}$. Among these five parameters in Eq. (1), w_0, n_0, and S_0 can be relatively easier to determine from empirical data for masses and radii of stable nuclei, while the remaining two parameters, K_0 and L, are more difficult to fix [11]. This is why we focus on the various sets of K_0 and L (Table 1) in analyzing neutron star matter.

These two parameters, K_0 and L, mainly determine the stiffness of neutron-rich nuclear matter, but have yet to be fixed. It is also suggested that K_0 is related to the giant resonances of stable nuclei [12], while L is associated with the structure and reactions of neutron-rich nuclei [7, 11, 13] and the pressure of pure neutron matter at the saturation density of SNM.

Additionally, one could constrain L via quasi-periodic oscillations in giant flares observed from soft-gamma repeaters [14, 15].

In contrast to the well-known empirical nuclear mass and radius formulas [16], the neutron star counterparts have to be theoretically given as function of not only the central density (ρ_c), but such EOS parameters as K_0 and L. So far, however, the dependence of low-mass neutron star models on K_0 and L remains to be examined systematically. We thus start with construction of the neutron star models from various EOSs of neutron star matter that meet the following conditions:

(1) Unified description of matter in the crust and core based on the same EOS of nuclear matter with specific values of K_0 and L.
(2) Consistency of the masses and radii of stable nuclei calculated within the same theoretical framework with the empirical values.

Mass and radius formulas for low-mass neutron stars are finally obtained in such a way as to approximately reproduce the neutron star models thus constructed.

2. Adopted EOS's of neutron star matter

Among many available EOSs of neutron star matter, we adopt the EOSs that meet the above conditions, i.e., unified EOSs, which are categorized into three groups as in Table 1. The first is based on the phenomenological EOS of uniform nuclear matter that was constructed by two of us [11], using a simplified version of the extended Thomas-Fermi theory [17], in such a way as to reproduce empirical masses and radii of stable nuclei. They adopted the Padé-type potential energies with respect to the nucleon density n_b for SNM and for neutron matter, respectively, and connected them in a quadratic approximation with respect to neutron excess α. This form of the potential energy can well reproduce the variational calculations of Friedman and Pandharipande [18], to which, in fact, the high-density behavior of neutron matter was adjusted. The α dependence of the potential energy is partially justified by the variational calculations of Lagaris and Pandharipande [19], and the expression for the total energy reproduces Eq. (1) in the limit of $n_b \to n_0$ and $\alpha \to 0$. With such EOSs of uniform nuclear matter obtained for various sets of (K_0, L), they constructed the EOSs of neutron star matter [20] by generalizing the above Thomas-Fermi theory as done by Oyamatsu [17]. Hereafter, such EOSs of neutron star matter are referred to as the OI-EOSs. We remark that generally accepted values of K_0 lie in the range of 230 ± 40 MeV [21] or so, while the OI-EOSs include rather extreme cases of $K_0 = 180$ and 360 MeV, as shown in Table 1, to cover the large parameter space. The final mass and radius formulas would remain almost unchanged even if the OI-EOSs with $K_0 = 180$ and 360 MeV are not included in the fitting.

In the second group, there are two EOSs of neutron star matter calculated within the relativistic framework. One is the Shen EOS based on the relativistic mean field theory with the TM1 nuclear interaction [22], and the other is the Miyatsu EOS based on the relativistic Hartree-Fock theory with the chiral quark-meson coupling model [23]. In both EOSs, the same type of the Thomas-Fermi model as used for the OI-EOSs is used in describing neutron star matter in such a way as to reproduce empirical masses and radii of stable nuclei.

The third group is composed of the five EOSs of neutron star matter based on the Skyrme-type effective interactions: FPS [24], SLy4 [25], BSk19, BSk20, and BSk21 [26–28]. The FPS

interaction, which was constructed by fitting the properties of uniform nucleon matter calculated by Friedman and Pandharipande [18], well reproduces the empirical ground-state properties of doubly magic stable nuclei via the Hartree-Fock calculations. The SLy4 interaction was constructed by Chabanat et al. [29] in such a way as to reproduce the microscopic EOS of neutron matter calculated with the UV14+UVII nuclear force by Wiringa, Fiks, and Fabrocini [30] as well as the empirical ground-state properties of doubly magic stable nuclei within the Hartree-Fock approximation. The BSk19, BSk20, and BSk21 interactions are written in the form of the nuclear energy-density functionals, which are derived from generalized Skyrme interactions in such a way as to fit all the available nuclear mass data [26]. As a result, empirical charge radii were also well reproduced. These interactions are different in the sense that BSk19, BSk20, and BSk21 are fitted to the EOSs of neutron matter derived by Friedman and Pandharipande [18], Akmal, Pandharipande, and Ravenhall [31], and Li and Schulze [32], respectively. This difference is expected to play a role in estimating the effect of uncertainties in three-neutron interactions on the stellar properties, as we shall see. In describing neutron star matter, a compressible liquid-drop approach was used for FPS and SLy4, while an extended Thomas-Fermi model was used for BSk19, BSk20 and BSk21. To calculate the neutron star models in the present study, we adopt the analytical expressions for FPS and SLy4 given by Haensel and Potekhin [33] and for BSk19, BSk20, and BSk21 given by Potekhin et al. [34].

3. Neutron star models

Now, we construct nonrotating neutron stars by integrating the Tolman-Oppenheimer-Volkoff equations from the stellar center of density ρ_c outward up to the position where the pressure vanishes. It is not clear up to what density the adopted unified EOSs are applicable. Nonetheless, one can expect that non-nucleonic components such as hyperons and quarks do not occur below $\sim 2\rho_0$ [1] and that the uncertainty from three-neutron interactions in the EOS of pure neutron matter becomes relevant above $\sim 2\rho_0$, as suggested by quantum Monte Carlo (QMC) calculations [35]. We thus examine the stellar models for $\rho_c \leq 2\rho_0$, where ρ_0 is set to 2.68×10^{14} g cm^{-3}, and the resultant M-R relations are plotted in Fig. 1(a).

To systematically describe various stellar models, we introduce a new auxiliary parameter η defined as $\eta = (K_0 L^2)^{1/3}$. The values of η are shown in Table 1. Remarkably, the M-R relation changes almost smoothly with η. Note that the OI-EOSs [20] with $L \lesssim 10$ MeV are too soft to keep the pressure positive and thus not used here. This implies the lower limit of η of order 30 MeV. Meanwhile, the EOS models used here cover the values of η up to ~ 200 MeV, which is significantly larger than expected from existing nuclear experiments. We remark that the powers of L and K_0 in η are chosen to be simple rational numbers in such a way that η has the same unit as L and K_0, i.e., MeV. If one considers arbitrary real numbers as the exponents, therefore, one could choose different kinds of η with which the M-R relation changes as smoothly as the present choice.

From the observational viewpoint, the radiation radius $R_\infty = R/\sqrt{1 - 2GM/Rc^2}$ and the gravitational redshift $z = 1/\sqrt{1 - 2GM/Rc^2} - 1$ with the gravitational constant G and the speed of light c could be more relevant in describing the stellar properties than M and R. The calculated z-R_∞ relation again shows a smooth change with η (Fig. 1(b)). The photon flux, if detected, would be proportional to $(R_\infty/D)^2$, where D is the distance from the
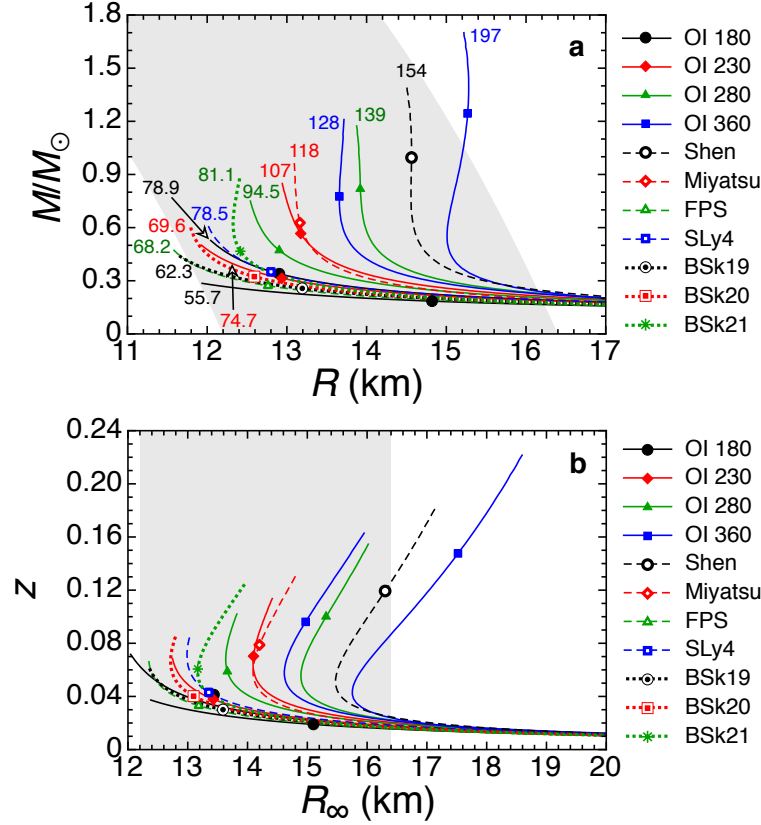
Fig. 1 Neutron star properties. The stellar models are constructed from various unified EOSs with different sets of (L, K_0). We plot the relations between the mass and radius (a) and between the gravitational redshift and radiation radius (b). The mark and end on each line denote the stellar models with $\rho_c = 1.5\rho_0$ and $2.0\rho_0$, respectively. In (a), the labels on the lines denote the values of the nuclear matter parameter η. To distinguish between the OI-EOSs, we add the values of K_0 to the OI-EOS labels; for example, we use "OI 180" for the two OI-EOSs with $K_0 = 180$ MeV (left, smaller L; right, larger L). The shaded region corresponds to the allowed region from the observed radiation radius of the neutron star in ω Cen (see text for details).

Earth, while the gravitational redshift could be determined from the possible shift of atomic absorption lines in spectra of the stars.

The smooth change of the stellar properties with η suggests that not only future nuclear experiments but also simultaneous measurements of M and R or, equivalently, z and R_∞ could constrain η, which could in turn lead to restriction of the stellar models. In particular, observations of low-mass neutron stars would be essential. For example, the radiation radius of the X-ray source, CXOU 132619.7–472910.8, in the globular cluster NGC 5139 (ω Cen) has been determined as $R_\infty = 14.3 \pm 2.1$ km from the *Chandra* data [36]. The allowed region from this R_∞ is shown in Fig. 1(a) and (b) with the shaded region. This is still consistent with various values of η, but future precise determination of R_∞ could constrain η, if M is low enough. Additionally, thermal spectra detected from quiescent low-mass X-ray binaries are expected to give M and R simultaneously [3, 4].
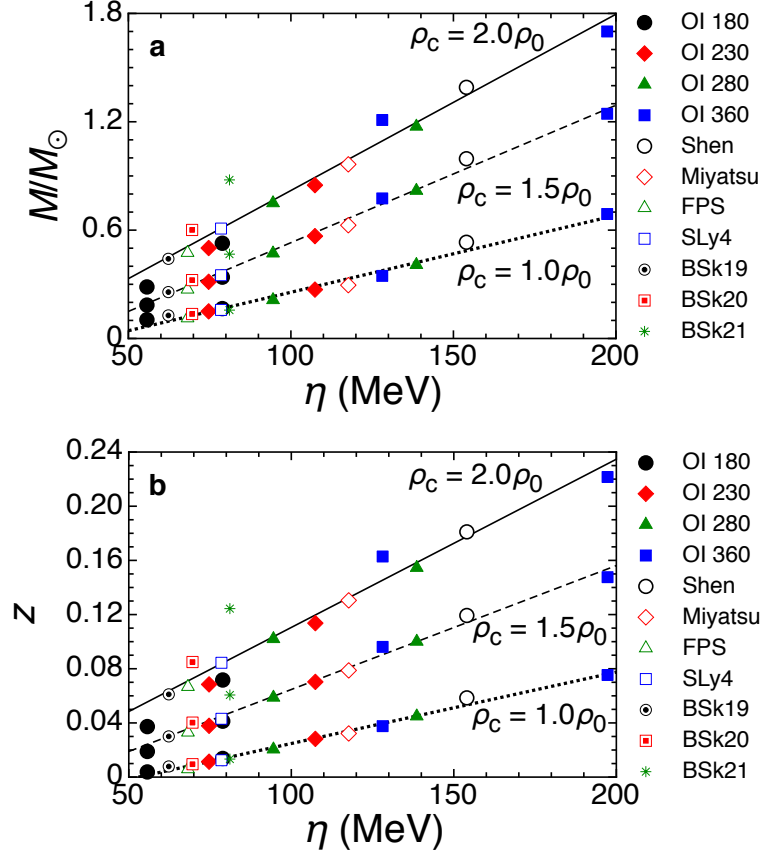
Fig. 2 Neutron star masses (a) and gravitational redshifts (b) as a function of η. The stellar models constructed from various unified EOSs are given for $\rho_c = 2.0\rho_0$, $1.5\rho_0$, and $1.0\rho_0$. The solid, broken, and dotted lines are the linear fitting to the cases of $\rho_c = 2.0\rho_0$, $1.5\rho_0$, and $1.0\rho_0$, respectively (see text for details).

4. Mass and radius formulas

To examine the dependence of the stellar properties on η more clearly, we plot the stellar masses calculated for $\rho_c = 2.0\rho_0$, $1.5\rho_0$, and $1.0\rho_0$ (Fig. 2(a)). From this figure, we find that the stellar masses for fixed ρ_c can be approximately expressed as a linear function of η, $M/M_\odot = c_0 + c_1(\eta/100\,\text{MeV})$, where c_0 and c_1 are adjustable parameters that depend on ρ_c. The validity of η is now evident. The deviation of the calculations from the linear fit at $\rho_c = 2.0\rho_0$ is larger than that at $\rho_c = 1.0\rho_0$, particularly for BSk20 and BSk21. Such deviation is of the order of uncertainties in M due to three-neutron interactions obtained from the QMC evaluations [35]. The parameters c_0 and c_1 can then be expressed as a quadratic function of $u_c \equiv \rho_c/\rho_0$ within the accuracy of errors less than a few percent (Fig. 3). Finally, we obtain the mass formula:

$$\frac{M}{M_\odot} = 0.371 - 0.820u_c + 0.279u_c^2 - (0.593 - 1.25u_c + 0.235u_c^2)\left(\frac{\eta}{100\,\text{MeV}}\right), \qquad (2)$$

where we confine ourselves to $\rho_c \gtrsim 0.9\rho_0$; otherwise, the stellar models can become unstable with respect to decompression, depending on the EOS of neutron star matter.
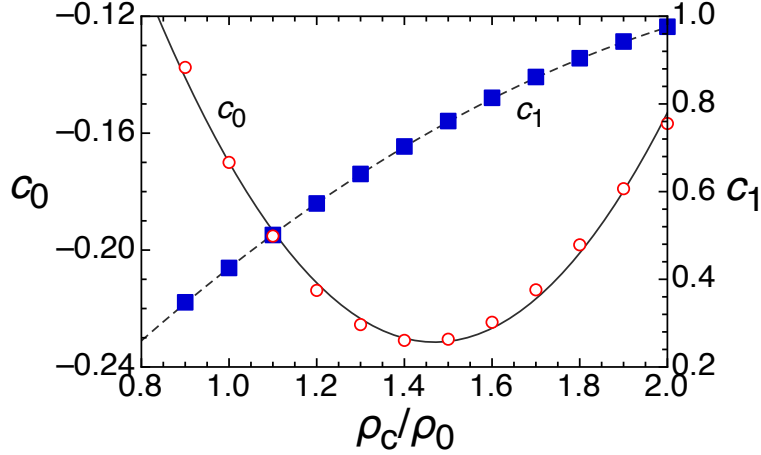
Fig. 3 Values (marks) of the adjustable parameters c_0 and c_1 in the mass formula. The corresponding quadratic fitting curves (solid and broken lines) are also shown as a function of ρ_c/ρ_0. Here we consider the stellar models only for $\rho_c \gtrsim 0.9\rho_0$ to avoid unstable neutron star models.

We also find that the gravitational redshift calculated for fixed ρ_c can be approximately expressed as a linear function of η (Fig. 2(b)). Then, just like the mass formula (2), we can obtain the theoretical formula for z as

$$z = 0.00859 - 0.0619u_c + 0.0255u_c^2 - (0.0429 - 0.108u_c + 0.0120u_c^2)\left(\frac{\eta}{100\,\text{MeV}}\right). \quad (3)$$

Using Eqs. (2) and (3), one could estimate the values of η and u_c from possible simultaneous measurements of M and z. In general, Eqs. (2) and (3) can have as many as four sets of solutions (u_c, η) for given observational values of $M/M_\odot$ and z. As mentioned above, however, Eqs. (2) and (3) are valid in the range of $0.9 \lesssim u_c \leq 2.0$. In this range, as shown in Fig. 2, the solution (u_c, η) has to be unique.

It is straightforward to obtain the formula for R from Eqs. (2) and (3). The obtained formula can be compared with the calculations of R for $\rho_c = 1.0\rho_0$, $1.5\rho_0$, and $2.0\rho_0$ (Fig. 4). We confirm a good agreement between those two except for $\eta \lesssim 70$ MeV. The mass and radius formulas could help to constrain not only the nuclear matter parameter η but also a star's ρ_c via possible simultaneous measurements of the star's M and R. If such measurements are precise, η could be deduced to within the accuracy of ± 20 MeV, which would provide a basis for analyzing more massive neutron stars.

From Fig. 4, one can also observe that the calculated R depends nonlinearly on ρ_c at small values of η, while converging on an approximately linear function of η at sufficiently large values of η:

$$R = 10.32 + 2.57\left(\frac{\eta}{100\,\text{MeV}}\right)\,\text{km}. \quad (4)$$

Note that such nonlinear dependence at small values of η arises from the flattened behavior of the corresponding M-R relations that can be seen from Fig. 1(a), while such convergence at large values of η is related to the vertically straightened behavior of the corresponding M-R relations.
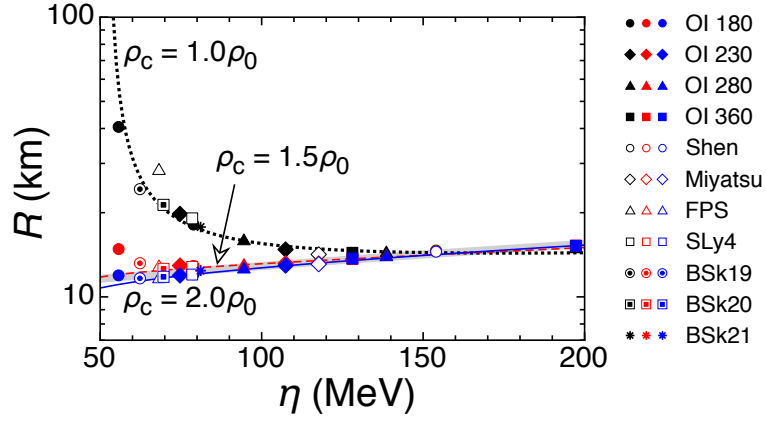
Fig. 4 Neutron star radii as a function of η. The stellar models constructed from various unified EOSs are given for $\rho_c = 1.0\rho_0$ (black), $1.5\rho_0$ (red), and $2.0\rho_0$ (blue). The solid, broken, and dotted lines are the formula values for the cases of $\rho_c = 2.0\rho_0$, $1.5\rho_0$, and $1.0\rho_0$, respectively, obtained from Eqs. (2) and (3). The thick straight line denotes the converging behavior expressed by Eq. (4).

5. Conclusion

In this paper, we have succeeded in constructing the theoretical formulas for the masses, gravitational redshifts, and radii of low-mass neutron stars as functions of the star's central density and the new EOS parameter η in a manner that is consistent with empirical masses and radii of stable nuclei. The value of η, which characterizes the stiffness of neutron star matter, remains unknown, but could be deduced from possible simultaneous M and R measurements via comparison with our formulas if the star observed is light enough. Thus, a firm evidence for the presence of low-mass neutron stars is first of all desired. One promising candidate is the neutron star in the high-mass X-ray binary 4U 1538-52, of which the mass could be significantly low or even the lowest among stars with known mass if the binary orbit is eccentric [37, 38]. The X-ray burster 4U 1724-307 in the globular cluster Terzan 2 is even more interesting because the X-ray data from the cooling phase of photospheric radius expansion bursts apparently allow the object to have a relatively low mass and still a significantly large radius [39]. Such conclusions are tentative partly because of the dependence on the atmosphere models adopted and partly because of uncertainties in the distance to the object, but, if valid, might eventually suggest the η value of order or even larger than 130 MeV.

Acknowledgment

References

[1] J. M. Lattimer and M. Prakash, Science **304**, 536 (2004).

[2] B. Kiziltan, A. Kottas, M. De Yoreo, and S. E. Thorsett, Astrophys. J. **778**, 66 (2013).

[3] S. Guillot, M. Servillat, N. A. Webb, and R. E. Rutledge, Astrophys. J. **772**, 7 (2013).

[4] J. M. Lattimer and A. W. Steiner, arXiv:1305.3242

[5] F. Özel, G. Baym, and T. Güver, Phys. Rev. D **82**, 101301 (2010).

[6] A. W. Steiner, J. M. Lattimer, and E. F. Brown, Astrophys. J. **765**, L5 (2013).

[7] M. B. Tsang et al., Phys. Rev. C **86**, 015803 (2012).

[8] P. B. Demorest, T. Pennucci, S. M. Ransom, M. S. E. Roberts, and J. W. T. Hessels, Nature **467**, 1081 (2010).

[9] J. M. Lattimer and M. Prakash, in From Nuclei to Stars: Festschrift in Honor of Gerald E Brown, ed. S. Lee (Singapore: World Scientific, 2011), 275

[10] J. M. Lattimer, Annu. Rev. Nucl. Part. Sci. **31**, 337 (1981).

[11] K. Oyamatsu and K. Iida, Prog. Theor. Phys. **109**, 631 (2003).

[12] J. P. Blaizot, Phys. Rep. **64**, 171 (1980).

[13] X. Roca-Maza, M. Centelles, X. Viñas, and M. Warda, Phys. Rev. Lett. **106**, 25250 (2011).

[14] H. Sotani, K. Nakazato, K. Iida, and K. Oyamatsu, Phys. Rev. Lett. **108**, 201101 (2012).

[15] H. Sotani, K. Nakazato, K. Iida, and K. Oyamatsu, Mon. Not. R. Astro. Soc. 428, L21 (2013).

[16] J. M. Blatt and V. F. Weisskopf, Theoretical Nuclear Physics (New York: Wiley, 1952).

[17] K. Oyamatsu, Nucl. Phys. A **561**, 431 (1993).

[18] B. Friedman and V. R. Pandharipande, Nucl. Phys. A **361**, 502 (1981).

[19] I. E. Lagaris and V. R. Pandharipande, Nucl. Phys. A **369**, 470 (1981).

[20] K. Oyamatsu and K. Iida, Phys. Rev. C **75**, 015801 (2007).

[21] E. Khan, J. Margueron, Phys. Rev. C **88**, 034319 (2013).

[22] H. Shen, H. Toki, K. Oyamatsu, and K. Sumiyoshi, Nucl. Phys. A **637**, 435 (1998).

[23] T. Miyatsu, S. Yamamuro, and K. Nakazato, Astrophys. J. **777**, 4 (2013).

[24] C. P.Lorenz, D. G. Ravenhall, and C. J. Pethick, Phys. Rev. Lett. **70**, 379 (1993).

[25] F. Douchin and P. Haensel, Astron. Astrophys. **380**, 151 (2001).

[26] S. Goriely, N. Chamel, and J. M. Pearson, Phys. Rev. C **82**, 035804 (2010).

[27] J. M. Pearson, S. Goriely, and N. Chamel, Phys. Rev. C **83**, 065810 (2011).

[28] J. M. Pearson, N. Chamel, S. Goriely, and C. Ducoin, Phys. Rev. C **85**, 065803 (2012).

[29] E. Chabanat, P. Bonche, P. Haensel, J. Meyer, and R. Schaeffer, Nucl. Phys. A **627**, 710 (1997).

[30] R. B. Wiringa, V. Fiks, and A. Fabrocini, Phys. Rev. C **38**, 1010 (1988).

[31] A. Akmal, V. R. Pandharipande, and D. G. Ravenhall, Phys. Rev. C **58**, 1804 (1998).

[32] Z. H. Li an H. J. Schulze, Phys. Rev. C **78**, 028801 (2008).

[33] P. Haensel, and A. Y. Potekhin, Astron. Astrphys. **428**, 191 (2004).

[34] A. Y. Potekhin, A. F. Fantina, N. Chamel, J. M. Pearson, and S. Goriely, Astron. Astrophys. in press (arXiv:1310.0049)

[35] S. Gandolfi, J. Carlson, and S. Reddy, Phys. Rev. C **85**, 032801 (2012).

[36] R. E. Rutledge, L. Bildsten, E. F. Brown, G. G. Pavlov, and V. E. Zavlin, Astrophys. J. **578**, 405 (2002).

[37] V. S. Petrov, E. A. Antokhina, and A. M. Cherepashchuk, Astron. Rep. **57**, 669 (2013).

[38] M. L. Rawls et al., Astrophys. J. **730**, 25 (2011).

[39] V. Suleimanov, J. Poutanen, M. Revnivtsev, and K. Werner, Astrophys. J. **742**, 122 (2011).